Renewable Energy 130 (2019) 1226–1236

Contents lists available at ScienceDirect

Renewable Energy

journal homepage: www.elsevier.com/locate/renene

Review

Strategy for wind power plant contribution to frequency control under variable wind speed

Pengfei Li [a], Weihao Hu [a, b, *], Rui Hu [a], Qi Huang [b], Jun Yao [c], Zhe Chen [a]

[a] Department of Energy Technology, Aalborg University, Aalborg 9220, Denmark
[b] School of Energy Science and Engineering, University of Electronic Science and Technology of China, Chengdu 611731, China
[c] State Key Laboratory of Power Transmission Equipment & System Security and New Technology, School of Electrical Engineering, Chongqing University, Chongqing 400044, China

A R T I C L E I N F O

Article history:
Received 23 March 2017
Received in revised form
9 November 2017
Accepted 12 December 2017
Available online 14 December 2017

Keywords:
Primary frequency control
Constraint command
De-loading control
Static frequency difference coefficient
Variable wind speed
Over-speeding control
Pitch control

A B S T R A C T

Current constraints require limiting the power transmitted from wind farms to power grids. Hence, wind turbine systems should be capable of regulating and limiting the generation capacity for a wide range of operating wind speeds. In addition, wind power plants must be endowed with active power and frequency control capabilities. In a single wind farm, wind turbines can be installed at different heights or altitudes, consequently exposing them to variable environmental conditions that can cause variations among their surrounding wind speeds. Thus, we propose a de-loading control strategy that integrates over-speeding and pitch control of wind turbines operating at variable wind speeds. This strategy allows not only storing power to satisfy the constraint demand of the power grid, but also contributing to primary frequency control. In fact, the proposed control strategy can adjust the static frequency difference coefficient of wind turbines, which is based on the proportion of variable-speed wind turbines operating under high wind speeds. Moreover, the proposed control strategy, which supports frequency control of the power grid under power constraints, suitably supports the frequency regulation of wind turbines that work at different wind speeds. Simulation results suggest that the proposed control strategy meets the power grid constraints, enhances the performance of primary frequency control, alleviates the frequency control pressure from thermal power plants, and appropriately generates curtailed wind power under variable wind speeds.

Contents

* Corresponding author. School of Energy Science and Engineering, University of Electronic Science and Technology of China, Chengdu 611731, China
E-mail address: whu@et.aau.dk (W. Hu).

https://doi.org/10.1016/j.renene.2017.12.046

P_{m}	Mechanical power of generator
C_{p}	Wind energy utilization coefficient
v	Wind speed
R	Blade radius
ρ	Air density
ω_{r}	Rotor speed of wind turbine
Λ	Tip speed ratio
B	Pitch angle
T_{m}	Mechanical torque of high-speed shaft
T_{e}	Electromagnetic torque of generator
ω_{g}	Rotational speed of generator
J	Rotational inertia of driving system
B	Coefficient of rotational viscosity
P_{e}	Electromagnetic power of generator
P_{v}	Maximum power of VSWT
P_{c}	Dispatching order value
P^{*}	Target active power
ω_{g}^{*}	Target generator speed
T_{e}^{*}	Target electromagnetic torque
n	Gearbox speedup ratio
v_{in}	Cut-in wind speed
v_{n}	Rated wind speed
v_{out}	Cut-out wind speed
λ_{opt}	Optimum tip speed ratio
ω_{lim}	Upper limit of rotational speed
d	Initial de-loading coefficient
Δf	Frequency deviation
P_{de}	Reference power in de-loading operation
P_{opt}	Reference power in maximum power tracking
$C_{\mathrm{p\text{-}de}}$	Wind energy utilization coefficient in de-loading operation
$C_{\mathrm{p\text{-}max}}$	Maximum wind energy utilization coefficient
λ_{d}	Tip speed ratio in de-loading operation
v_{d}	Upper limit of wind speed in over-speeding control
λ_{ref}	Reference tip speed ratio in over-speeding control
k'_{opt}	Tracking proportional coefficient of power curve in de-loading operation
β_{ref}	Reference pitch angle in de-loading control
P_{rated}	Rated power
P_{avail}	Maximum captured power
k_{d}	Natural de-loading coefficient
$C_{\mathrm{p\text{-}rated}}$	Wind energy utilization coefficient when wind turbine works at rated power
β_{rated}	Reference value of pitch angle when wind turbine work at rated power
P_{T}	Adjustable active power of wind power plant (WPP)
P_{ref}	Power constraint from power grid to WPP
$P_{\mathrm{WT\text{-}i}}$	Reference power for *i*th wind turbine
ΔP_{i}	Active power of *i*th wind turbine to be adjusted under specific constraint
$P_{\mathrm{opt\text{-}i}}$	Reference power for *i*th wind turbine in maximum power tracking
$\Delta P_{\mathrm{i}}^{\mathrm{AB}}$	Adjustable active power of *i*th wind turbine type A or B
$\Delta P_{\mathrm{i\text{-}res}}^{\mathrm{AB}}$	Reserved active power of *i*th wind turbine type A or B in de-loading operation
$P_{\mathrm{C\text{-}res}}$	Sum of reserved power for type C wind turbines
$P_{\mathrm{AB\text{-}res}}$	Sum of reserved power for type A and B wind turbines
$P_{\mathrm{ABC\text{-}res}}$	Sum of de-loading reserved power for WPP
$\Delta P_{\mathrm{i}}^{\mathrm{C}}$	Adjustable active power of *i*th wind turbine type C
R_{W}	Frequency difference coefficient of wind turbine
H_{m}	Proportion of wind turbines operating at high wind speed
P_{f}	Sum of additional power adjustment values
P_{WT}	Reference power for WPP
D'	Real value of the wind turbine de-loading coefficient

1. Introduction

LARGE-SCALE integration of wind power sources into the power grid causes fluctuation and randomness that notably affects frequency control and peak shaving in the power system [1,2]. Results in Refs. [3–5] show that wind power is becoming economically suitable in some parts of the world, such as the United States and the Northwest and Northeast regions of China. However, complications with wind energy curtailment appear in these places, and the proportion of wind-based generation is limited to 20%

of the total power in the grid [6]. Moreover, given the problems associated with wind power curtailment and the difficulty to consume the generated wind power in large-scale integrated systems, different scales of power constraints are imposed by the power grid [7,8]. Overall, it is imperative to both improve the frequency regulation capability of wind power plants (WPPs) and adequately use the curtailed wind power. By solving these problems, WPPs could be used as the primary frequency regulation reserve and to optimize wind energy consumption.

In recent years, several studies have been presented on active power control, where primary frequency control is performed in WPPs. For instance [9,10], present a constrained-mode optimized control strategy that aims to prevent the frequent activation and deactivation of wind turbines and reduce the amount of pitch angle changes. This strategy could ensure a safe, stable, and economic operation of a WPP under the load-limitation mode in the power grid; however, it did not consider frequency control. In Refs. [11,12], the authors use wind turbines and storage systems to perform frequency coordination control, which can employ the storage systems as frequency reserve and enhance the frequency control characteristics of wind turbines. However, the storage systems currently have several drawbacks, such as small capacity and high cost. Other studies are focused on the characteristics of wind turbines. In Refs. [13,14], it is proposed a virtual inertia control to contribute in primary frequency control by releasing kinetic energy of the rotor. Nevertheless, this kind of method can only support frequency response for a short time and may cause a frequency drop when the wind turbines stop controlling frequency. Wang, Yi, et al. [15] use an adaptive de-loading control method that employs a part of the available active power to serve as frequency regulation reserve for power systems.

Given that either the wind turbines can be located at different heights in a single WPP or a group of WPPs can be located at different altitudes in the same area, variable wind speeds can affect their operation. Regarding economical aspects of wind power generation, the authors in Ref. [16] proposed a strategy that considers a part of the wind turbines to operate under high wind speeds for primary frequency control by using de-loading operation. When a considerable proportion of wind turbines operate at high wind speeds, this strategy can satisfy the requirements of both frequency control and economy, provided the wind power generation is not restricted by the power grid. However, this approach is not convenient for primary frequency control when most of the wind turbines operate at low wind speeds. Moreover, the coordination and optimization of all the WPP resources is difficult to achieve for satisfying the constraints and frequency control requirements of a power system. Consequently, plenty of research on frequency control focuses only on either active power control or maximum power point tracking (MPPT). However, there is scarce work on a coordinative control for power and frequency regulation aiming to meet the comprehensive requirements of the power grid.

In this paper, we propose an integrated control strategy for power and frequency control that is based on constraint demands and variable wind speeds acting on the turbines. First, we present a coordinative de-loading control method that merges over-speeding and pitch control, and considers variable wind speed. In addition, we propose a frequency control scheme based on the adjustment of the difference coefficient, which is related to the proportion of wind turbines operating at high wind speeds. Furthermore, this control scheme uses a power distribution strategy to prioritize the use of wind turbines operating at high wind speeds, complies with the constraints imposed by the power grid, and applies frequency control to support the power grid operation under variable wind speeds. We verified the validity of the proposed frequency control strategy by simulating a power system that includes a WPP and a thermal power plant.

2. Active power control for WPPs

In this section, we present the models for active power control of a WPP, variable-speed wind turbine (VSWT) generator, improved pitch control, and active power system of VSWT under the normal operating condition.

2.1. Active power control system

Considering the WPP requirements of grid frequency control and peak shaving, its active power control system should consist of three operational levels, as shown in Fig. 1. They include wind energy management, WPP control, and wind turbine control.

Fig. 1 shows that the comprehensive active power control allows a WPP operation under different frequency modes, such as normal and constrained modes imposed by the power grid. Hence, the appropriate mode can be selected according to the different power grid requirements.

2.2. Simplified VSWT model

Wind turbines depend on blades to capture wind and convert its energy into mechanical torque at the hub. Then, a gearbox increases the main-shaft speed and transmits the mechanical energy to a generator via the gearbox. Finally, the generator, which we consider to be a doubly fed induction generator (DFIG), converts the mechanical torque into electrical energy, as depicted in Fig. 2.

Considering the energy loss and transmission efficiency, the mechanical power at the DFIG side is given by

$$P_{\mathrm{m}} = \frac{1}{2}\rho A C_{\mathrm{p}} v^3 = \frac{1}{2}\rho \pi R^2 C_{\mathrm{p}}(\lambda, \beta) v^3, \tag{1}$$

$$\lambda = \frac{\omega_{\mathrm{r}} R}{v}, \tag{2}$$

where P_{m} is the mechanical power of the generator, C_{p} is the wind energy utilization coefficient, v is the wind speed, R is the blade

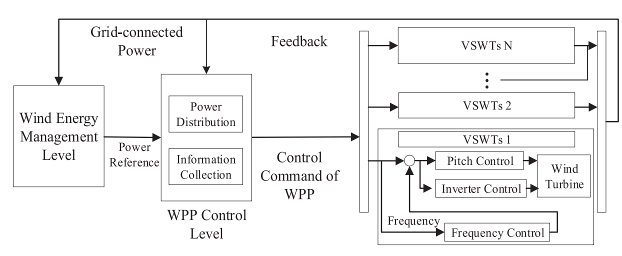

Fig. 1. Diagram of active power control for a WPP.

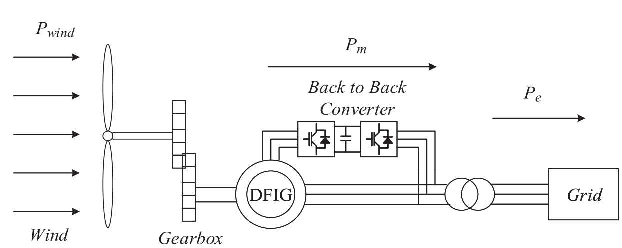

Fig. 2. Wind energy conversion process.

radius, ρ is the air density, ω_r is the rotor speed of the wind turbine, λ is the tip speed ratio, and β is the pitch angle.

From equation (1), for constant wind speed v and air density ρ, the absorbed power from the rotor only depends on coefficient C_p. Therefore, the active power of a VSWT can be adjusted by varying C_p [17], which is a high-order nonlinear function and can be determined by

$$C_p(\lambda,\beta) = 0.22\left(\frac{116}{\lambda_1} - 0.4\beta - 5\right)e^{-\frac{12.5}{\lambda_1}}, \tag{3}$$

$$\frac{1}{\lambda_1} = \frac{1}{\lambda + 0.08\beta} - \frac{0.035}{\beta^3 + 1}. \tag{4}$$

Thus, C_p depends only on tip speed ratio λ and pitch angle β when the wind speed is constant.

In addition, VSWTs can operate at a constant frequency under variable wind speed, and hence decouples its rotational speed from the grid frequency. Furthermore, VSWTs suitably operate under a wide range of wind speeds (this range usually handles variations of ±30%) and use ac excitation of the rotor to compensate the difference between mechanical rotation and synchronous speed. Hence, the frequency of the stator can be adjusted to match that of the grid. Moreover, the application of vector control for generators has allowed the decoupling of active and reactive power control in large-scale wind turbines. Therefore, a VSWT model can be simplified as illustrated in Fig. 3 and defined as follows.

$$T_m = \frac{P_m}{\omega_g} = \frac{\pi\rho R^3 C_p(\lambda,\beta)v^2}{2\lambda}, \tag{5}$$

where T_m and T_e are the mechanical torque of the high-speed shaft and the electromagnetic torque of the generator, respectively, and ω_g is the rotational speed of the generator.

The VSWT drive train model can be expressed as

$$\omega_g = \frac{1}{J}\int(T_m - T_e - B\omega_g)dt, \tag{6}$$

where J is the rotational inertia of the driving system and B is the coefficient of rotational viscosity.

Thus, the electromagnetic power of the generator P_e can be determined by

$$P_e = T_e\omega_g. \tag{7}$$

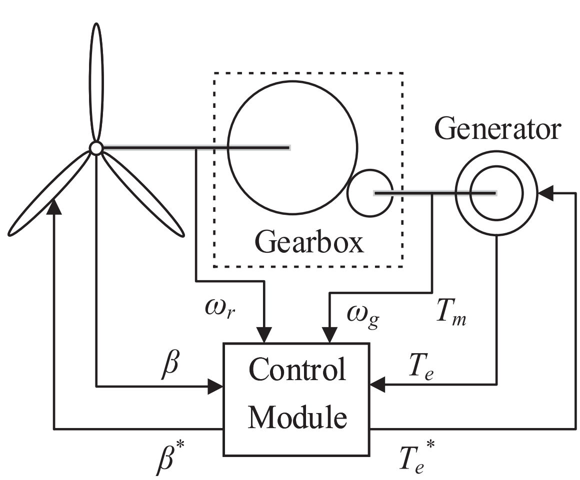

Fig. 3. VSWT simplified diagram.

Consequently, the VSWT control requires references of active power P^*, generator speed ω_g^*, and electromagnetic torque T_e^*.

According to its operating curve, the maximum power of a VSWT, P_v, which is calculated from the current wind speed, and the dispatching order value for the VSWT, P_c, which depends on the WPP and the required active power, allow to determine $P^* = \min(P_v, P_c)$.

The reference generator speed, ω_g^*, can be calculated by the following control strategy:

$$\omega_g^* = \begin{cases} \dfrac{\lambda_{opt} v n}{R}, & v_{in} \le v \le v_n \\ \omega_{g\max}, & v_n \le v \le v_{out} \end{cases}, \tag{8}$$

where n is the gearbox speedup ratio, v_{in}, v_n, and v_{out} are the cut-in, rated, and cut-out wind speeds of the VSWT, respectively. There are two cases for a VSWT to operate under either constrained power or MPPT when there is no constraint. The VSWT can operate with optimum tip speed ratio λ_{opt} in the range of wind speed $v_{in} \le v \le v_n$, whereas it should operate at the upper limit of rotational speed, $\omega_{g\,max}$, in the range $v_n \le v \le v_{out}$.

The electromagnetic torque can be set as

$$T_e^* = P^* \big/ \omega_g^*. \tag{9}$$

However, given the large rotational inertia of VSWTs, the rotational speed cannot be quickly changed to follow either the wind speed or a changing reference for active power. Thus, the active power response can be delayed and the control process can present chattering. To prevent these situations, we set electromagnetic torque T_e^* as

$$T_e^* = P^* \Big/ \sqrt{\omega_g^* \omega_g}. \tag{10}$$

The reference for the pitch angle in conventional pitch control is given by the deviation between rotational speed of wind turbine ω_r and upper limit of rotational speed ω_{lim}. In contrast, we propose an improved pitch control that considers additional control elements for frequency to control the generated power of the WPP and additional power for primary frequency control. In addition, we calculated the reference value of the pitch angle, β_{ref}, using a specific module. The diagram of the proposed pitch control that satisfies the comprehensive requirements of the power grid is shown in Fig. 4.

The WPP uses both de-loading and frequency control when generation is constrained by the power system. When the transmission system of the wind turbine is replaced by a first-order mass model, the wind turbine is given by the model illustrated in Fig. 5.

The decision module of the wind turbine accepts different parameters, such as initial de-loading coefficient d from the WPP control level, reference power for the wind turbine P_{WT}, static frequency difference coefficient R_w of the wind turbine, and frequency deviation Δf. In addition, the wind turbine should meet the constraints imposed by the power system to participate in primary

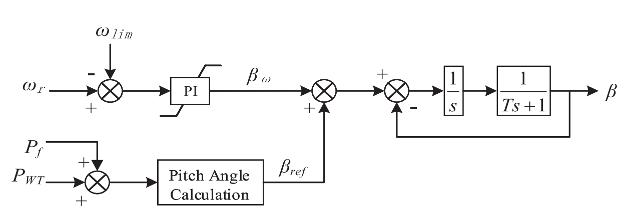

Fig. 4. Improved pitch control system.

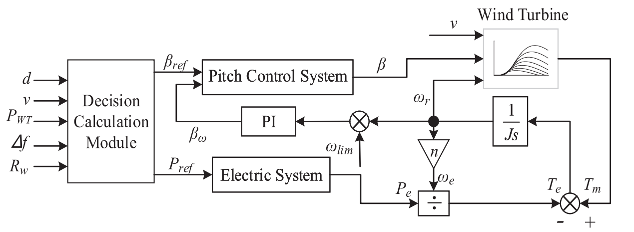

Fig. 5. Active power control system for a VSWT with generation constrained by the power system.

frequency control by calculating the corresponding reference values of pitch angle β_{ref} and electromagnetic power P_{ref}.

3. Proposed WPP frequency control under power system constraints

3.1. De-loading control of wind turbines

For a single wind turbine, if the de-loading coefficient is set to $0 \leq d \leq 1$, the following references can be determined:

$$P_{\text{de}} = (1-d)P_{\text{opt}} = 0.5\rho\pi R^2 C_{\text{p-de}} v^3, \tag{11}$$

$$P_{\text{opt}} = 0.5\rho\pi R^2 C_{\text{p-max}} v^3, \tag{12}$$

where P_{de} and P_{opt} are the references for power under de-loading operation and power for MPPT, respectively, $C_{\text{p-de}}$ is the wind energy utilization coefficient in de-loading operation, and $C_{\text{p-max}}$ is the maximum wind energy utilization coefficient.

When wind speed v and air density ρ are constant, and from equations (11) and (12), coefficient $C_{\text{p-de}}$ can be calculated by

$$C_{\text{p-de}} = (1-d)C_{\text{p-max}}. \tag{13}$$

Equation (13) shows that if the wind energy utilization coefficient decreases in a rate of d, the de-loading operation of the wind turbines can be realized. Fig. 6 shows that for a given wind speed v_0, the wind energy utilization coefficient varies according to the pitch angle from β_0 to β_1. In addition, the de-loading control of wind turbines can be realized by increasing the rotating speed from optimized rotating speed ω_0 to speed ω_1. Over-speeding and deceleration control can realize the de-loading operation of a WPP to decrease the load. However, the over-speeding control allows the kinetic energy of the rotor to be stored as spinning reserve. Thus, over-speeding control is convenient for de-loading control.

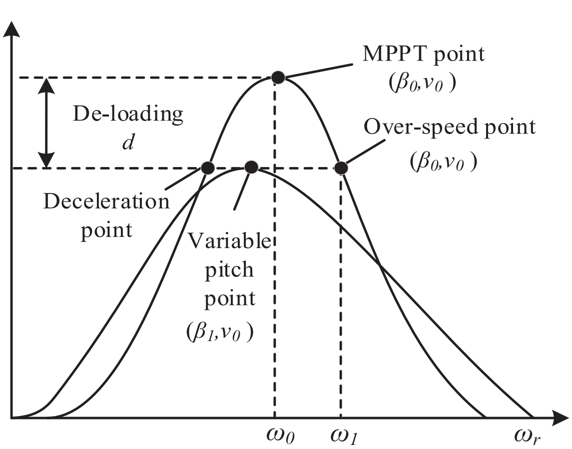

Fig. 6. Principle of de-loading control for wind turbines.

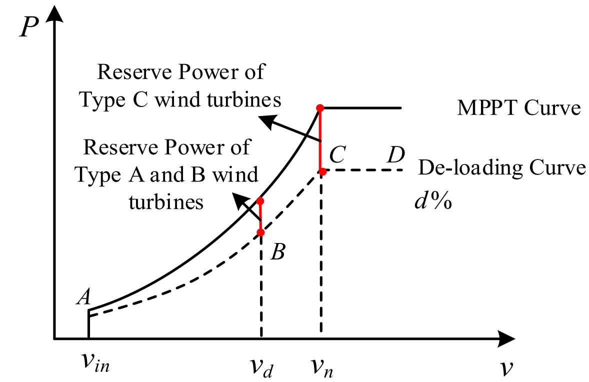

Fig. 7. De-loading power curve of wind turbines according to wind speed.

Given the uncertainties related to wind speed, the wind turbines in a WPP might operate at different speeds. Fig. 7 shows the de-loading power curve of wind turbines according to the wind speed. We classified wind turbines in a WPP into three types, namely, A, B, and C, according to the wind speed at which they operate. Thus, types A, B, and C wind turbines operate in the wind speed intervals AB, BC, and CD, respectively, as shown in Fig. 7. This classification allows to take full advantage of the capabilities and usable range of over-speeding and pitch control by using different de-loading control strategies. Specifically, we perform de-loading operation by using over-speeding control for type A, integrated de-loading control by using over-speeding and pitch control for type B, and de-loading operation by using pitch control for type C.

In type A, the wind turbines operate at low wind speeds comprised between v_{in} and v_{d}, where the latter represents the upper limit of wind speed at which the turbines can use over-speeding control to achieve de-loading operation at rate d. Hence, the relationship between the wind energy utilization coefficient in de-loading operation and its maximum value can be determined by

$$C_{p-de}(\lambda_d, 0) = (1-d)C_{p-max}(\lambda_{opt}, 0), \tag{14}$$

where λ_{d} is the tip speed ratio under de-loading operation.

Thus, to determine the tuning range, ratio λ_{d} can be calculated from a lookup table based on the C_{p}–λ–β curve. Furthermore, according to the following equation of the tip speed ratio under de-loading operation:

$$\lambda_d = \omega_{\max} R / v_d, \tag{15}$$

the maximum wind speed for over-speeding control v_{d}, can be calculated when the initial de-loading coefficient is d. In this case, the reference parameters for stable operation are: $\beta = 0$ and $\omega_{\text{ref}} = \lambda_{\text{ref}} \cdot v/R$, where λ_{ref} is the reference tip speed ratio for over-speeding control. From equation (14), after calculating $C_{\text{p-de}}(\lambda_{\text{ref}}, 0)$, ratio λ_{ref} can be calculated using the lookup table with a pitch angle of 0°.

Then, considering equations (2) and (11), the reference power under de-loading operation can be calculated as

$$P_{\text{de}} = 0.5\rho A R^3 C_{\text{p-de}} \omega^3 \Big/ \lambda_{\text{d}}^3, \tag{16}$$

and considering equations (8) and (11), it can be calculated as

$$P_{\text{de}} = 0.5\rho A R^3 (1-d) C_{\text{p-max}} \omega^3 \Big/ \lambda_{\text{ref}}^3 = k'_{\text{opt}} \omega^3, \tag{17}$$

where k'_{opt} is the tracking proportional coefficient of the power curve under de-loading operation, which is given by

$$k'_{opt} = 0.5\rho AR^3(1-d)C_{p-max}\Big/\lambda_{ref}^3. \tag{18}$$

Thus, the reference power under de-loading operation can obtained from equation (17).

In type B, the wind turbines operate at middle wind speeds, in the range between v_d and v_n, and the dependency only on over-speeding control does not satisfy the required d for de-loading operation. In fact, when the rotational speed reaches its upper limit by using over-speeding control, pitch control is required to accomplish de-loading operation. In this case, the calculation method of the reference power is the same as that used for type A, and the other reference values for stable operation are: $\beta = \beta_{ref}$, $\omega_{ref} = \omega_{max}$, and $\lambda_{ref} = \omega_{max}R/v$, where β_{ref} is the reference pitch angle for de-loading operation. Coefficient $C_{p\text{-}de}(\lambda_{ref},\beta_{ref})$ can be calculated as

$$C_{p-de}\left(\lambda_{ref},\beta_{ref}\right) = (1-d)C_{p-max}(\lambda_{opt},0). \tag{19}$$

In type C, the wind turbines operate at high wind speeds between v_n and v_{out}. In this range, only pitch control can be used to realize de-loading operation, and the reference values for stable operation are: $\beta = \beta_{ref}$, $\omega_{ref} = \omega_{max}$, $\lambda_{ref} = \omega_{max}R/v$, and $P_{ref} = (1-d)P_{rated}$.

We also introduce natural de-loading coefficient k_d that represents the ratio between rated power P_{rated}, when wind turbines work above the rated wind speed, and maximum captured power P_{avail} as follows:

$$k_d = \frac{P_{rated}}{P_{avail}} = \frac{0.5\rho\pi R^2 C_{p-rated}v^3}{0.5\rho\pi R^2 C_{p-max}v^3}. \tag{20}$$

The wind energy utilization coefficient at a high wind speed for de-loading operation can be determined by

$$C_{p-de}\left(\lambda_{ref},\beta_{ref}\right) = (1-d)C_{p-rated}\left(\lambda_{ref},\beta_{rated}\right), \tag{21}$$

where $C_{p\text{-}rated}$ and β_{rated} are, respectively, the wind energy utilization coefficient and the reference pitch angle when the wind turbines operate at the rated power.

Combining equation (21) with equations (19) and (20) we obtain

$$C_{p-de}\left(\lambda_{ref},\beta_{ref}\right) = (1-d)k_d C_{p-max}(\lambda_{opt},0). \tag{22}$$

3.2. Power distribution over WPP

When the power grid imposes constraints on the WPP to guarantee power and frequency regulation reserves, the WPP requires an initial de-loading operation at rate d. Hence, we considered that the wind turbines operating under different wind speeds are de-loaded at rate d. Thus, we avoided including additional scheduling control for wind turbines when using different de-loading coefficients [18,19]. After the WPP stabilizes under the initial de-loading operation, it switches to the constrained operation.

Under the constraining commands of the power grid, the adjusted active power to meet the required load limitation can be expressed as

$$P_T = P_{ref} - (1-d)P_{opt}, \tag{23}$$

where the P_T is the active power of the WPP to be adjusted and P_{ref} is the power constraint imposed to the WPP from the power grid.

The reference power for the ith wind turbine is given by

$$P_{WT-i} = \Delta P_i + (1-d)P_{opt-i}, \tag{24}$$

where ΔP_i is the active power of the ith wind turbine that needs to be adjusted to the constraint and $P_{opt\text{-}i}$ is the reference under MPPT.

In Fig. 7, the de-loading operation of wind turbines at different wind speeds produces variations in the reserved power. We aimed to operate as few wind turbines as possible under load limitation and increase the frequency regulation reserve with turbines working at low wind speeds that contribute to primary frequency control. Therefore, given that type C wind turbines reserve more active power than those in the other types, we prioritized them to perform any scheduled load limitation, followed by type B and finally type A wind turbines. This allocation scheme is processed for each type of wind turbine according to the amount of reserved active power. For either a type A or type B wind turbine [20], the power adjustment in de-loading operation is determined by

$$\Delta P_i^{AB} = \begin{cases} 0;P_T \le P_{C-res} \\ \dfrac{P_{i-res}^{AB}}{P_{AB-res}}(P_T - P_{C-res});P_{C-res} < P_T \le P_{ABC-res} \end{cases}, \tag{25}$$

where $\Delta P_{i\text{-}res}^{AB}$ is the reserved active power of the ith type A or B wind turbine for de-loading operation, $P_{C\text{-}res}$, $P_{AB\text{-}res}$, and $P_{ABC\text{-}res}$ are the sums of reserved power among type C, type A and type B, and all the wind turbines in the WPP, respectively.

The power adjustment for a type C wind turbine in de-loading operation is determined by

$$\Delta P_i^{C} = \begin{cases} \dfrac{P_{i-res}^{C}}{P_{C-res}}P_T;P_T \le P_{C-res} \\ P_{i-res}^{C};P_{C-res} < P_T \le P_{ABC-res} \end{cases}. \tag{26}$$

From equations (24)–(26), it is possible to calculate reference power $P_{WT\text{-}i}$ for every wind turbine command by the WPP to operate under the constraints imposed by the power grid.

3.3. Static frequency difference coefficient of wind turbines

To filter minor signal disturbances, traditional turbines are endowed with a frequency regulation deadband. Likewise, wind turbines require a deadband, particularly when they contribute to frequency control. Our proposed frequency control strategy aims to ensure that every wind turbine contributes to frequency regulation without depending on its working condition. Moreover, we aim to fully utilize the reserved wind energy in the presence of load limitation. Thus, we set a deadband for the wind turbines in any working condition to be 0.02 Hz [21]. In addition, we considered that the value of the static frequency difference coefficient has a substantial effect on the primary frequency control of a power system. According to the power droop curve of a traditional generator, a variable frequency difference coefficient of wind turbine, R_W, should be introduced. Compared with the fixed regulation coefficient, this frequency difference coefficient can result in a more suitable frequency support from wind turbines [22].

Therefore, we propose a method to adjust the static frequency difference coefficient that is based on the proportion of wind turbines operating at high wind speeds in the WPP. We used a line to represent the relationship between the static frequency difference coefficient of wind turbines and the proportion of wind turbines operating at high wind speeds in the WPP. Based on this relationship, the static frequency difference coefficient can be determined, as illustrated in Fig. 8.

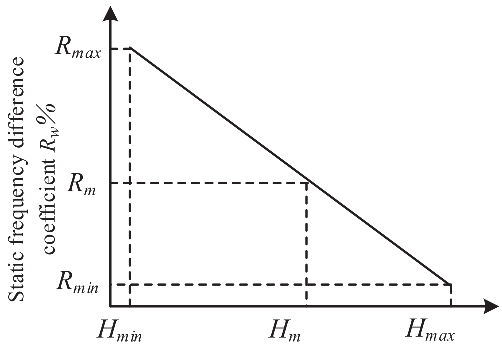

Fig. 8. Regulation coefficient according to the proportion of wind turbines operating at high wind speeds.

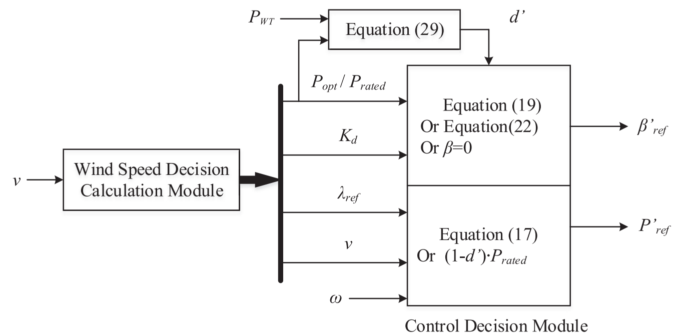

Fig. 9. Calculation of control parameters for a wind turbine.

This coefficient plays an important role in maintaining the frequency stability of the power system, because small coefficient values imply strong frequency stability. However, in real operating conditions, a very small static frequency difference coefficient will lead to an unreasonable load distribution among the generators in the power system.

For instance, the static frequency difference coefficient should range between 2% and 5% in a thermal turbine. In this range, the frequency response has a suitable performance. Hence, we also set the static frequency difference coefficient of wind turbines to be in this range, and it can be calculated as follows:

$$R_W = R_{\min} + \frac{R_{\max} - R_{\min}}{H_{\max} - H_{\min}}(H_{\max} - H_m), \tag{27}$$

where H_m is the proportion of wind turbines operating at high wind speeds, $R_{\min} = 2\%$, $R_{\max} = 5\%$, $H_{\min} = 0\%$, and $H_{\max} = 100\%$.

3.4. Frequency control of wind turbines

The decoupled control between active and reactive power of a VSWT implies the independence between the rotational speed of the turbine and the power grid frequency. Therefore, the wind turbine cannot respond to the primary frequency control of the power grid under normal working conditions. Hence, an additional frequency controller for active power is required to take full advantage of the wind energy under constrained operation and enhance the frequency characteristics for primary frequency control. The additional active power required by the frequency deviation can be expressed as

$$P_f = -\frac{1}{R_W}\Delta f. \tag{28}$$

Under constrained operation and when a frequency variation occurs, the reference for active power of the wind turbine corresponds to the sum of power P_f and reference power P_{WT} from the WPP. Thus, the real de-loading coefficient d' of the wind turbine can be calculated as

$$d' = \begin{cases} 1 - \dfrac{P_{WT} + P_f}{P_{opt}}; v \le v_n \\ 1 - \dfrac{P_{WT} + P_f}{P_{rated}}; v > v_n \end{cases}. \tag{29}$$

For frequency control of a WPP, coefficient d' can be obtained from equation (29), and the reference values for pitch control and the electrical system in frequency control can be determined by replacing d by d' in the corresponding equations. Consequently, the control requirements for frequency control of the power grid can be met by using these references. Fig. 9 shows the calculation of the different parameters for the wind turbine control that represent the decision modules for wind speed and control.

4. Simulations and analyses

4.1. Simulated power system

To verify the effectiveness and correctness of the proposed control strategy for primary frequency in a WPP, we performed simulations using the MATLAB Simulink software and implemented the model shown in Fig. 10. This model includes a 600 MW thermal power plant, a 150 MW WPP composed of 100 wind turbines with a power of 1.5 MW per turbine, and a load of 650 MW [23]. In addition, we considered the following parameters for the power system: $R_m = 0.05$, $T_{GT} = 0.02$ s, $F_{HP} = .3$, $T_{RH} = 7$ s, $T_{CH} = 0.3$ s, $H = 5$ s, and $D = 1$.

For us to represent wind turbines operating at different wind speeds, we selected three different wind speeds corresponding to the abovementioned types of wind turbines: 8.5 m/s for type A wind turbines, 11 m/s for type B wind turbines, and 14 m/s for type C wind turbines. In addition, given that type B wind turbines use the control strategies of both types A and C wind turbines, we omitted them from the simulation to clearly show the effect of frequency control using the proposed strategies. Moreover, we considered that the initial load corresponds to the generated power in the simulation, and the initial frequency of the power system was set to $f = 50$ Hz, the initial de-loading level of the WPP to $d = 0.2$, the constraint on the WPP imposed by the power system to 90 MW, and the schedule command of the thermal power plant to 560 MW. At time $t = 60$ s, the system load was suddenly increased by 20 MW. We evaluated two cases for the WPP operation, one when most of the wind turbines work at low wind speed, and the other when most of the wind turbines work at high wind speed, as detailed in Table 1.

4.2. Analysis of simulation cases

4.2.1. Frequency control when most turbines operate at low wind speed

For Case 1, we compared two situations, namely, when the WPP does and does not participate in frequency control based on the proposed control strategy. The corresponding simulation results are shown in Fig. 11.

Fig. 11 shows that when the frequency change occurs, the output power of both the WPP and thermal power plant increases when the system frequency drops, provided that the WPP participates in frequency control. The proposed control strategy performs a variety

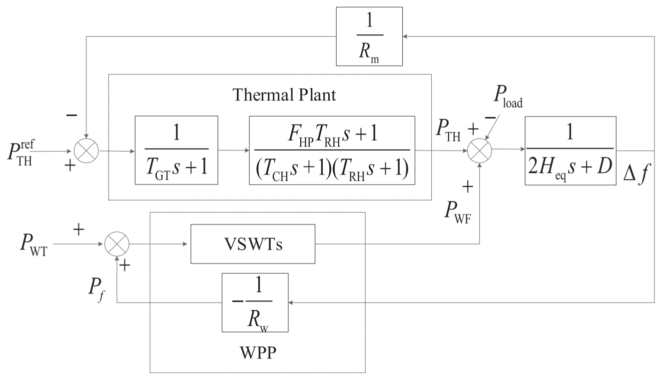

Fig. 10. Power system model to simulate primary frequency control.

of de-loading strategies. For instance, the frequency reserve is used in various working conditions, and when the frequency suddenly changes, the type A wind turbines release their rotational kinetic energy stored in the rotors by reducing the speed of the generator. This releasing can quickly provide active power support for the power system. Likewise, the type C wind turbines capture more wind energy by reducing the pitch angle, which is based on the frequency variation, to provide frequency support for the power system. When the load changes after 60 s, the frequency response of the power system tends to stabilize. However, given that the primary frequency control deviates the regulation, the frequency does not return to 50 Hz afterwards. This situation can be compensated by using a secondary frequency control.

The output response of the thermal power plant in Fig. 11 shows a transient drop due to the WPP active power support to the power

Table 1
Parameters of the evaluated cases for WPP operation.

Case	Number of type C wind turbines	Proportion of type C wind turbines (%)	Static frequency difference coefficient (%)	Maximum WPP output power (MW)
Case 1	40	40	3.8	104.3
Case 2	80	80	2.6	134.7

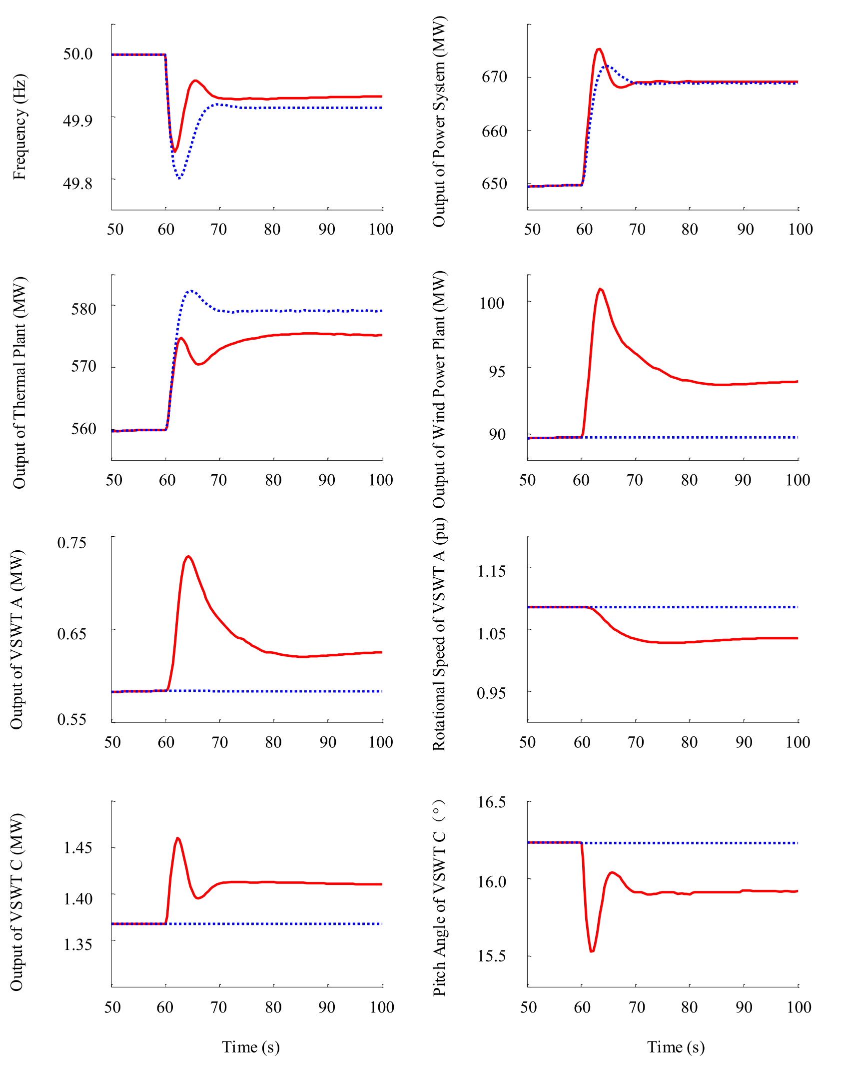

Fig. 11. Parameters response when most wind turbines operate at low wind speed.

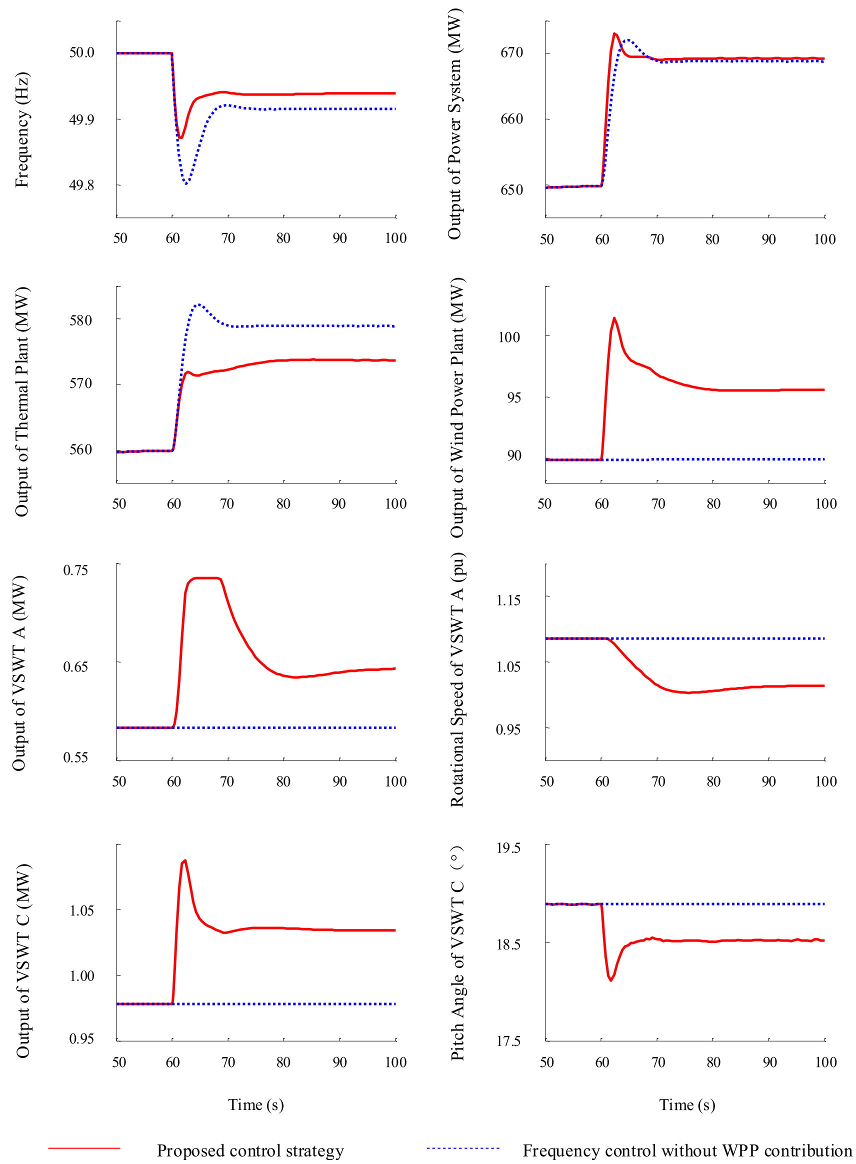

Fig. 12. Parameters response when most wind turbines operate at high wind speed.

system. This phenomenon is caused by the fast power response of wind turbines to the increase in the load, and the thermal plant power returns to a stable level after the output power of the WPP decreases. Compared with the situation when the WPP does not contribute to frequency control, its contribution can quickly reduce the frequency drop and provide frequency support to the power system. Furthermore, this could reduce the pressure on the thermal power plant contribution to frequency control.

4.2.2. Frequency control when most turbines operate at high wind speed

Similar to Case 1, in Case 2 we compared the two situations when the WPP does and does not participate in frequency control. The corresponding simulation results are shown in Fig. 12. The figure shows that when the frequency change occurs, types A and C wind turbines reduce, respectively, their rotational speed and pitch angle to provide the frequency support for the power system. Given that the static frequency difference coefficient reduces, the output power of type C wind turbines increases. Thus, the output power of the thermal plant does not present a considerable reduction and smoothly rises to a stable value.

4.3. Frequency control performance

Table 2 lists characteristics of the frequency control for different simulation cases. Example 1 is WPP operating under rated wind speed; Example 2 and Example 3 are the proposed frequency control when most of the wind turbines operate at low and high wind speeds, respectively. Compared with Example 1, both

Table 2
Primary frequency control performance for different cases.

Example	Maximum frequency drop (Hz)	Deviation from target frequency (Hz)	Output power of thermal plant (MW)
Example 1	49.80	0.09	19.2
Example 2	49.84	0.07	15.3
Example 3	49.87	0.06	13.7

Example 2 and Example 3 show smaller maximum frequency drop and deviation from the target frequency of the power system. Moreover, there is a reduction of the thermal power plant contribution to frequency control. In Example 2 and Example 3, for a constant power constraint, the proposed frequency control enhances the regulation performance when most of the wind turbines operate at high wind speed. Furthermore, this control can reduce the output power of the thermal power plant and make significant use of the reserved wind energy in de-loading operation.

To further evaluate the impact of the static frequency difference coefficient on frequency control and its underlying principles, we varied the coefficient using three different settings and compared the corresponding results. The three settings we used for the static frequency difference coefficient were: 2%, 5%, and the use of the proposed static frequency difference coefficient. Furthermore, we considered the four scenarios detailed in Table 3. Fig. 13 shows the frequency response for the different simulation scenarios and coefficient settings.

In Fig. 13(1), in the scenario where the wind turbines have no power limitation and most of them operate at a low wind speed, a small static frequency difference coefficient implies an increased contribution in the frequency control of the WPP to the power system. However, the frequency fluctuation of the power system will increase, and thus decrease its stability. In Fig. 13(2), in the scenario where the wind turbines have a power limitation and most of them operate at a low wind speed, a small static frequency difference coefficient might lead to a deteriorated frequency control. When the coefficient is 2%, there appears a transient stable frequency between 65 s and 71 s followed by a frequency drop. Overall, the frequency response when the static difference coefficient is 2% presents shorter peaks and reduced fluctuation in Fig. 13(3) and (4) than in Fig. 13(1) and (2). In Scenario 4 (Fig. 13(4)), the presence of power limitation does not impact the frequency response of the power system, because type A wind turbines represent a small proportion in the WPP. Thus, the power response when most of the wind turbines operate at low wind speed has a negligible impact on the frequency control performance of the power system. Comparing the frequency response using the proposed static frequency difference coefficient with that using a coefficient of 5% in the different simulation scenarios, we found that the frequency control stability with the 5% coefficient is better than that with the proposed static frequency difference coefficient, but the frequency control contribution is higher using the proposed frequency control. Thus, considering all the operating conditions of the WPP, we conclude that adjusting the static frequency difference coefficient in real time can balance stability and economy, and provide a satisfying frequency control.

Table 3
Primary frequency control scenarios.

Scenario	Conditions
Scenario 1	Most of the wind turbines operate at low wind speed No maximum power limitation
Scenario 2	Most of the wind turbines operate at low wind speed Maximum power limitation
Scenario 3	Most of the wind turbines operate at high wind speed No maximum power limitation
Scenario 4	Most of the wind turbines operate at high wind speed Maximum power limitation

5. Conclusion

In this paper, we propose a control strategy for coordinating active power scheduling control and frequency control. The strategy is based on active power de-loading control of a WPP and adjusting the static frequency difference coefficient of wind turbines. In addition, the proposed method considers constraints in power requirements and wind turbines operating at variable wind speeds. The latter consideration applies for onshore WPPs in different geographical locations, especially at different altitudes, such as mountains and hills. The proposed control strategy allows a WPP to satisfy requirements of frequency control and power grid dispatching. According to the theoretical and simulation analyses

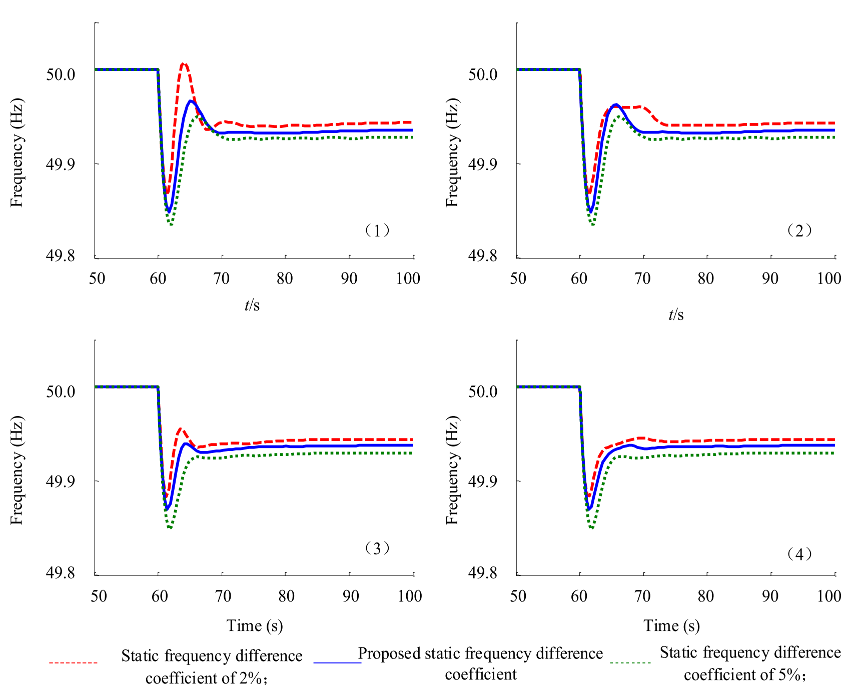

Fig. 13. Frequency response for different simulation scenarios.

presented in this paper, we can summarize the contributions and outcomes as follows:

1 Different de-loading control strategies were deduced for wind turbines operating in a wide range of wind speeds. The proposed control strategy can transfer the curtailed wind energy to the available frequency regulation reserve under constraints imposed by the power grid. In addition, this strategy thoroughly considers the operating characteristics of wind turbines to be applied in over-speeding and pitch control. At low wind speeds, the wind turbines only use over-speeding control to perform power de-loading operation without modifying the pitch angle. Hence, the proposed control strategy reduces pitch adjustment actions of the wind turbines under load limitation.
2 The power distribution strategy of wind turbines prioritize those operating at high wind speeds to participate in load-limitation and primary frequency control. Thus, the wind turbines take full advantage of their frequency regulation capabilities to meet the constraint requirements from the power grid. Furthermore, the proposed strategy can ensure the frequency control reserve in wind turbines operating at low wind speeds for the subsequent contribution to frequency regulation.
3 Given that power constraints are imposed by the power grid, a WPP can use the proposed control method to adjust the static frequency difference coefficient of wind turbines according to its own operating conditions. This frequency regulation strategy aids to balance the stability and economy in the power system when the WPP contributes to frequency control. Moreover, the control strategy can improve frequency control and decrease the control pressure on thermal power plants in the power system.

Acknowledgment

This work was supported by the by National Natural Science Foundation of China (51707029) and the Visiting Scholarship of State Key Laboratory of Power Transmission Equipment & System Security and New Technology (Chongqing University) (2007DA10512716402).

References

[1] Hannele Holttinen, et al., Impacts of large amounts of wind power on design and operation of power systems, results of IEA collaboration, Wind Energy 14 (2) (2011) 179–192.
[2] Dennis Y.C. Leung, Yuan Yang, Wind energy development and its environmental impact: a review, Renew. Sustain. Energy Rev. 16 (1) (2012) 1031–1039.
[3] Sari Fink, et al., Wind energy curtailment case studies. NREL subcontract report, NREL/SR-550 46716, 2009.
[4] Lori Bird, Jaquelin Cochran, Xi Wang, Wind and solar energy curtailment: experience and practices in the United States, NREL (2014), NREL/TP-6A20-60983.
[5] John Kabouris, Costas D. Vournas, Application of interruptible contracts to increase wind-power penetration in congested areas, IEEE Trans. Power Syst. 19 (3) (2004) 1642–1649.
[6] Chinese Wind Energy Association, 2011 Primary statistics on the wind power limitation[J], Wind Energy 3 (4) (2012) 1–4 (in Chinese).
[7] A.D. Hansen, P. Sorensen, F. Iov, et al., Centralised power control of wind farm with doubly fed induction generators[J], Renew. Energy 31 (7) (2006) 935–951.
[8] Stavros A. Papathanassiou, Nikos G. Boulaxis, Power loads and energy yield evaluation for wind farms operating in island systems, Renew. Energy 31 (4) (2006) 457–479.
[9] Lin Li, Xie Yongjun, Zhu Chenchen, Wang Ningbo, Priority list-based output-restricted active power control strategy for wind farms[J], Power Syst. Technol. 37 (4) (2013) 960–966 (in Chinese).
[10] Haoran Zhao, et al., Optimal active power control of a wind farm equipped with energy storage system based on distributed model predictive control, IET Gener. Transm. Distrib. 10 (3) (2016) 669–677.
[11] G.O. Suvire, P.E. Mercado, Active power control of a flywheel energy storage system for wind energy applications, IET Renew. Power Gener. 6 (1) (2012) 9–16.
[12] Haoran Zhao, et al., Optimal active power control of a wind farm equipped with energy storage system based on distributed model predictive control, IET Gener. Transm. Distrib. 10.3 (2016) 669–677.
[13] Ioannis D. Margaris, et al., Frequency control in autonomous power systems with high wind power penetration, IEEE Trans. Software Eng. 3.2 (2012) 189–199.
[14] Xue Yingcheng, Tai Nengling, Review of contribution to frequency control through variable speed wind turbine, Renew. Energy 36 (6) (2011) 1671–1677.
[15] Yi Wang, et al., Control of PMSG-based wind turbines for system inertial response and power oscillation damping, IEEE Trans. Software Eng. 6.2 (2015) 565–574.
[16] Wu Zishuang, Yu Jilai, Peng Xiyun, DFIG's frequency regulation method only for high wind speed with suboptimal power tracking[J], Trans. China Electrotech. Soc. 28 (5) (2013) 112–119 (in Chinese).
[17] Smart Grid Handbook, first ed., Wiley, New York, 2016, pp. 577–578.
[18] L.R. Chang-Chien, C.C. Sun, Y.J. Yeh, Modeling of wind farm participation in AGC[J], IEEE Trans. Power Syst. 29 (3) (2014) 1204–1211.
[19] R.G. De Almeida, J. Lopes, Participation of doubly fed induction wind generators in system frequency regulation[J], IEEE Trans. Power Syst. 22 (3) (2007) 944–950.
[20] K.V. Vidyanandan, N. Senroy, Primary frequency regulation by deloaded wind turbines using variable droop[J], IEEE Trans. Power Syst. 28 (2) (2013) 837–846.
[21] J.L. Rodriguez-Amenedo, S. Arnalte, J.C. Burgos, Automatic generation control of a wind farm with variable speed wind turbines[J], IEEE Trans. Energy Convers. 17 (2) (2002) 279–284.
[22] F. Diaz Gonzalez, M. Hau, A. Sumper, et al., Participation of wind power plants in system frequency control: review of grid code requirements and control methods[J], Renew. Sustain. Energy Rev. 34 (2014) 551–564.
[23] P. Kundur, Power System Stability and Control[M], McGraw-Hill, New York, 1994.